APPLICATION OF TWO-DIMENSIONAL CORRELATION SPECTROSCOPY FOR MONITORING THE MECHANISM OF REACTION BETWEEN PHENYL GLYCIDYL ETHER (PGE) AND METAPHENYLENE DIAMINE (MPDA)

by

MICHAEL R. HOLLOCK

B.S, Lehigh University, 1998

A REPORT

submitted in partial fulfillment of the requirements for the degree

MASTER OF SCIENCE

Department of Chemical Engineering
College of Engineering

KANSAS STATE UNIVERSITY
Manhattan, Kansas

2012

Approved by:

Major Professor
J. R. Schlup

Copyright

Abstract

The curing reaction for the amine epoxy resin system of phenyl glycidyl ether (PGE) with metaphenylene diamine (mPDA) was investigated using two-dimensional correlation spectroscopy in the near-infared region (2DNIR). Synchronous and asynchronous correlation maps were generated using 2Dshige© software. The characteristic NIR band assignments were made, including the identification of new peaks for the O-H combination band in the 4825-4750 cm^{-1} region and the C-H stretching vibration overtone at 6018 cm^{-1}. Finally, the data suggests the reaction proceeds as follows: the appearance of the OH groups and C-H backbone vibrations occurs before the primary amine and epoxide rings disappear.

Table of Contents

List of Figures

List of Tables

List of Equations

Supporting Files

Data_Hollock2012_calculations.xlsx
Data_FuSchlup1993_raw.csv

Acknowledgements

I would like to acknowledge Belinda Thompson at Honeywell Federal Manufacturing & Technologies for her encouragement to pursue my Master of Science in Chemical Engineering degree.

Additionally, without the ongoing support of J. R. Schlup at Kansas State University to keep me on task, this paper would not be possible.

Dedication

To Jennifer and Alyssa, thank you for accepting all the late hours and the countless extensions, but most of all, thank you for not letting me get discouraged.

Introduction

With a wide range of thermal and mechanical properties (Garcia, 2010), amine-based epoxies can be found in a plethora of applications such as adhesives, composites, coatings, and resins for commercial, aeronautical, and electrical industries (Pham, 2005). Real-time monitoring of the epoxy cure reaction provides valuable insight into the chemical and physical changes undergone by the species during polymerization. *In-situ* data can help in optimizing process and control parameters for the formulation and manufacture of epoxies.

Due to their vast array of uses, epoxy resins have been studied since their debut using a myriad of analytical techniques. Lettieri and Frigione (2005) placed the techniques into two categories: *in*d*irect* and *direct.* Indirect methods monitor a physical property associated with the conversion of the reactants as a function of time. These techniques include differential scanning calorimetry (DSC) (Barral, et al., 2000), rheology (Farquharson, Smith, & Shaw, 2002), ultrasonics (Aggelis & Paipetis, 2012) and photoluminescence (Gallot-lavallee, Teyssedre, Laurent, & Rowe, 2005). In direct methods, the concentration of reactive groups is measured as a function of time. Raman spectroscopy (Merad, et al., 2009; Swier, Assche, & Mele, 2004; Karkanas & Partridge, 1996), nuclear magnetic resonance (NMR) (Vargas, Sachsenheimer, & Guthausen, 2012), and Fourier-transform infrared (FTIR) spectroscopy (Cakic, Ristic, Jaso, Radicevic, Ilic, & Simendic, 2012; Kortaberria, Arruti, Gabilondo, & Mondragon, 2004) are included in this group. FTIR has commonly been employed in the mid-infrared (MIR) range since the functional groups involved in the epoxy/amine curing reaction have strong characteristic absorption peaks in this region of the spectrum (Musto, Mascia, Ragosta, Scarinzi, & Villano, 2000). However it has been shown that NIR is better suited than mid-infrared (MIR) spectroscopy for characterizing the epoxy/resin cure process (St. John & George, 1992; Min, Stachurski, Hodgkin, & Heath, 1993; Fu & Schlup, 1993; Xu, Fu, & Schlup, 1994). MIR spectra of epoxy resins and hardeners are very complex; primary and secondary amine and hydroxyl group absorptions are difficult to resolve from other functional group absorptions. Additionally, the costs of associated transmission fibers for remote sensing of *in situ* reaction monitor for NIR data collection is relatively cheaper and have lower attenuation losses than those used in MIR monitoring (Xu, Fu, & Schlup, 1996; Mijovic & Andelic, 1995).

Two-dimensional Correlation Analysis

For general two-dimensional (2D) correlation analysis, an external perturbation such as a chemical reaction is applied to a system. Data is collected systematically (i.e., spectral intensity as a function of time) and converted into a 2D correlation map through cross-correlation analysis (Noda & Ozaki, 2004). Dating back only two decades, the application of 2D correlation spectroscopy to the NIR region (2DNIR) is still in its infancy since being pioneered by Noda (1993) and others (Noda, Dowrey, Marcott, Story, & Ozaki, 2000). 2DNIR analysis simplifies complex spectra by sharpening and better resolving overlapping peaks and probes the sequential order of physical events within the system (Noda & Ozaki, 2004). Since the majority of spectral work conducted on epoxy/amine systems has historically focused on the MIR region, references for spectral band assignment in the 4000 cm^{-1} to 10000 cm^{-1} NIR spectrum are limited.

The reaction of between phenyl glycidyl ether (PGE) and metaphenylene diamine (mPDA) can serve as a great stepping-stone for the application of 2DNIR. The reaction involves a simple system of liquid reactants with no solvent interference. Their chemical structures are shown in figures 1 and 2, as well as a simplified reaction in figure 3. Since PGE is a monofunctional resin with a single reactive epoxide group, polymerization does not occur as it reacts with the multifunctional curing agent mPDA. *In-situ* NIR data on this system allows for focusing on specific overtones that are strong NIR energy absorbers. Fu and Schlup (1993) first used NIR to examine the disappearance of the epoxide ring. As the reaction of PGE and mPDA proceeds, the active hydrogens on the amine groups open the epoxide ring to form a hydroxyl group. Fu and Schlup (1993) found that this chemical change manifests itself at specific NIR peaks. The terminal epoxide group combination band and stretch overtone occur at 4534 and 6076 cm^{-1}, respectively. Primary amine combination occurs at 5058 cm^{-1}, while the primary amine and secondary amine overtones are seen at 6652 and 6641 cm^{-1}, respectively. Finally, the hydroxide stretch overtone appears at 6968 cm^{-1}. These band assignments are shown in Table 1.

Table 1. Characteristic NIR peaks for cured PGE/mPDA (Fu & Schlup, 1993)

Position (cm^{-1})	Assignment
4534	Terminal epoxide group combination
5052	Primary amine combination
5969	Aromatic C-H overtone
6076	Terminal epoxy ring stretch
6641	Secondary amine overtone
6652	Primary amine overtone
6968	O-H stretch overtone

Later Xu, Fu, & Schlup (1994) investigated the cure mechanism in detail and found that the path of the reaction using PGE and N-methylaniline follows three distinct steps: (1) formation of hydrogen-bonded epoxides or amines, (2) the formation of termolecular intermediates involving epoxides, amines, and hydroxyls, and (3) the decomposition of such intermediates through epoxide ring cleavage. Xu, Fu and Schlup (1996) applied NIR attenuated total reflectance (ATR) monitoring to the system in order to determine the feasibility of using ATR as an alternative sensor. Xu, Fu, and Schlup (1996) further analyzed the kinetics of a multifunctional epoxy/amine system using NIR to show that the reactions are autocatalytic and proposed a corresponding kinetic model. Xu and Schlup (1997) studied etherification versus amine addition for epoxy resin/amine cure reactions using tetraglycidyl 4,4'-diaminophenylmethane (TGDDM) and methylaniline (mAnil).

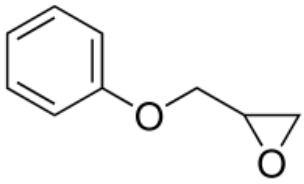

Figure 1. Chemical structure of PGE.

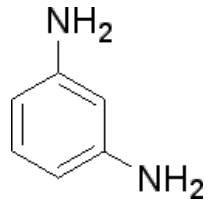

Figure 2. Chemical structure of mPDA.

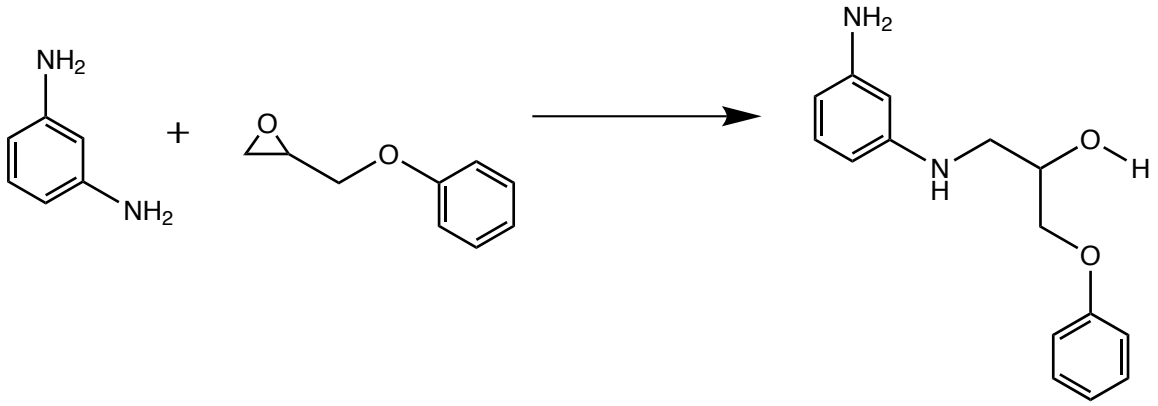

Figure 3. Simplified reaction of mPDA and PGE.

Although Schlup, et.al. (1993, 1994, 1996, and1997) examined the reaction of PGE and mPDA in great detail, no physical interpretation through 2DNIR has been completed to date on this specific system. With respect to thermosetting epoxy resins, Amari and Ozaki (2002) first used 2DNIR and ATR to monitor the initial oligomerization of bis-hydroxyl terepthalate (BHET). The authors found 2DNIR useful for *in situ* monitoring of water content in the reaction system. Li, Wu, Li, and Wu (2008) completed an extensive 2DNIR study of diglycidyl ether of bisphenol A (DGEBA) cured with 4,4'-diaminophenylmethane (DDM) and showed that both the amine and epoxy groups changed simultaneously during curing and took place prior to changes in the hydroxyl groups and CH_2/CH backbone changes. It is evident that the application of 2DNIR to thermosetting polymers has not been thoroughly studied. This lack of information presents favorable research opportunities. The application of 2DNIR to the PGE-mPDA system lays the foundation for future studies utilizing 2DNIR software on more complicated epoxy/resin systems.

Experimental

In Situ Near-IR Spectroscopy

The data in this report is a subset of that reported by Fu and Schlup (1993). The solution of reacting monomers was prepared by dissolving mPDA directly into liquid PGE at room temperature at a 3:1 mass ratio. After placing the solution in a Spectratech high temperature transmission cell, a background spectrum (t = 0 min) was obtained using a Mattson Instruments NOVA CYGNI 120 spectrometer with a tungsten halogen source, a quartz beamsplitter, and an indium antimonide detector. Absorbance data were subsequently collected from T=0 to T=192 min in the 4000 cm^{-1} to 8000 cm^{-1} NIR region; however, only the subset T=22 to T=182 data were used in this paper.

Two-dimensional Correlation Analysis

Generalized 2D correlation spectra were created using 2Dshige© Version 1.3 (Morita, 2005) software. This program performs cross-correlation analysis using Forward Fourier Transforms (FFT) of the absorbance data with respect to time using Equation 1. The synchronous map is generated from the real component and the synchronous map is generated from the imaginary component.

Equation 1. Generalized 2D correlation function.

$$\Phi(\nu_1, \nu_2) + i\psi(\nu_1, \nu_2) = \frac{1}{\pi(T_{max} - T_{min})} \int_0^\infty \tilde{Y}_1(\omega) \cdot \tilde{Y}_2^*(\omega) d\omega$$

As with any computational software, the data must be formatted correctly for use with the program and can prove to be one of the largest barriers to using the software. Although the program can analyze raw data, its authors recommend using averaged dynamic spectra. Raw absorbance data from Fu and Schlup (1993) data were averaged using a customary reference spectrum (Noda & Ozaki, 2004) where:

Equation 2. Reference spectrum.

$$\bar{y}(\upsilon) = \frac{1}{T_{max} - T_{min}} \int_{T_{min}}^{T_{max}} y(\upsilon, t) dt$$

The dynamic spectrum was then calculated using*:*

Equation 3. Dynamic spectrum.

$$\tilde{y}(\upsilon) = y(\upsilon, t) - \bar{y}(\upsilon)$$

Selected absorbance spectra (22, 102, and 182 min) shown in Fig. 4, giving an indication of some of the peaks identified by Fu and Schlup (1993). Fig. 5 shows the 0 to 42 min data in more detail. Note how the spectra for the 2 and 12 min periods are significantly shifted with

respect to the rest of the absorbance spectra. Such a shift can create noise in 2D correlation maps, since the software falsely associates a perturbation at these intervals. Using the 2 and 12 min data, the correlation map in Fig. 6 demonstrates several artificial peaks caused by the data shift. Fig. 7 shows the same map created without the 2 and 12 min data. For clarity, all of the 2DNIR maps generated using the 2Dshige© software for this report omitted the data collected at 0, 2 and 12 min.

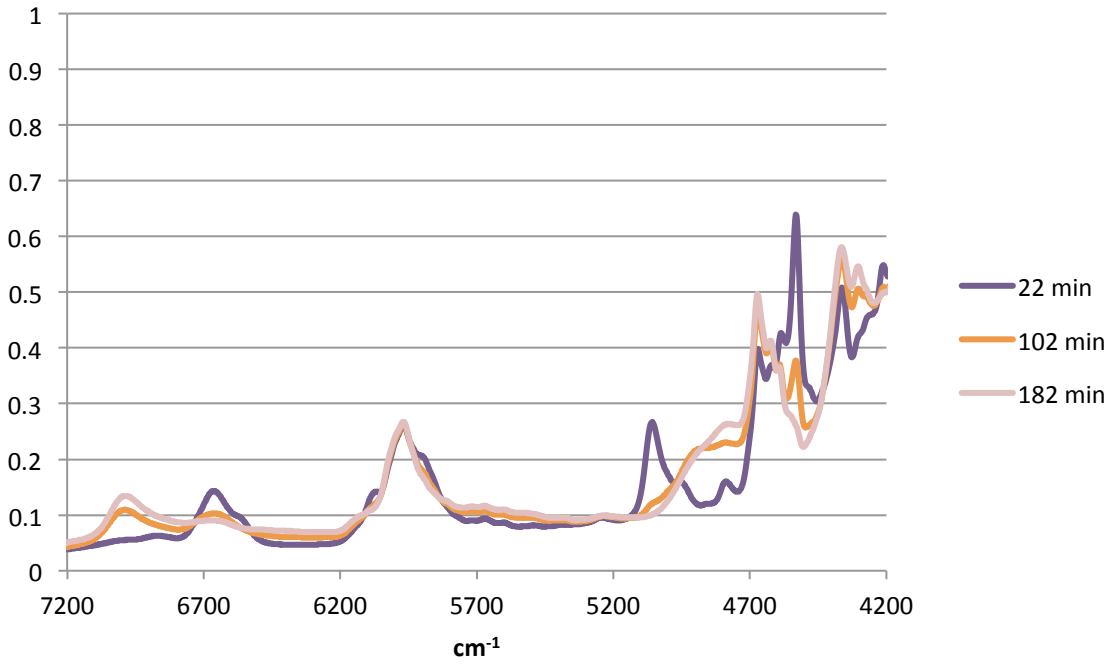

Figure 4. Absorbance data for PGE/mPDA at 75°C.

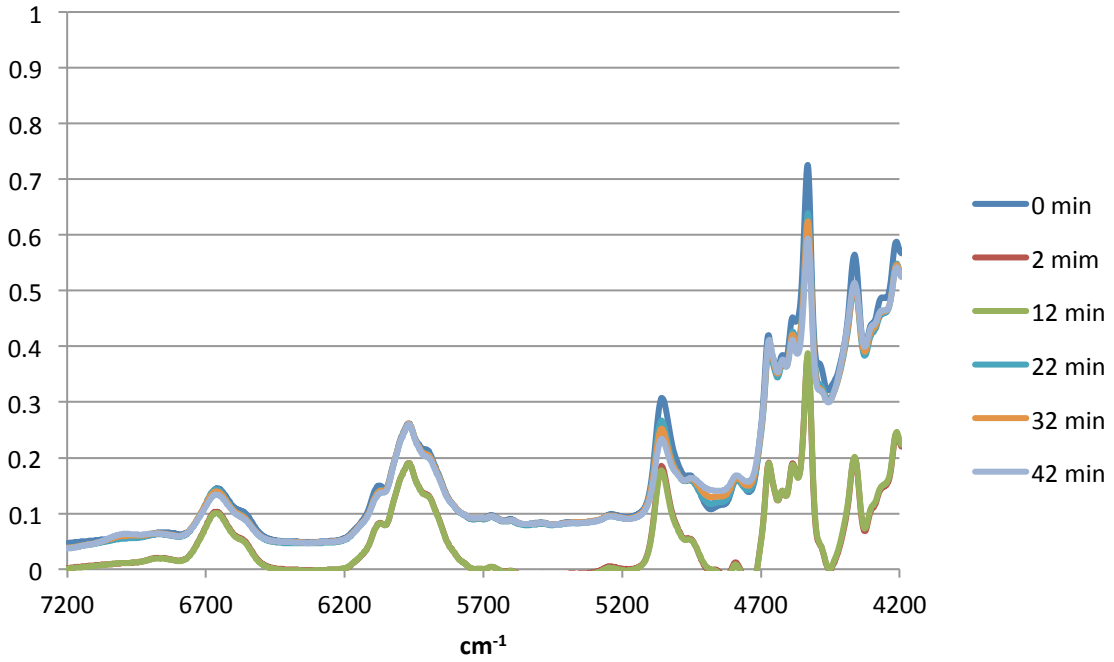

Figure 5. Absorbance data showing 2 and 12 min spectra shift.

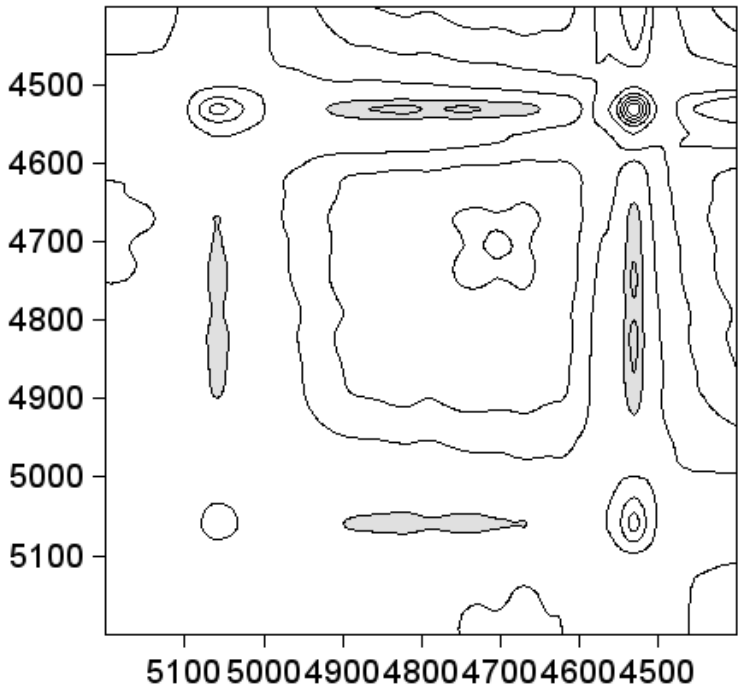

Figure 6. Synchronous map in the 5200-5400 cm^{-1} region with outlier data.

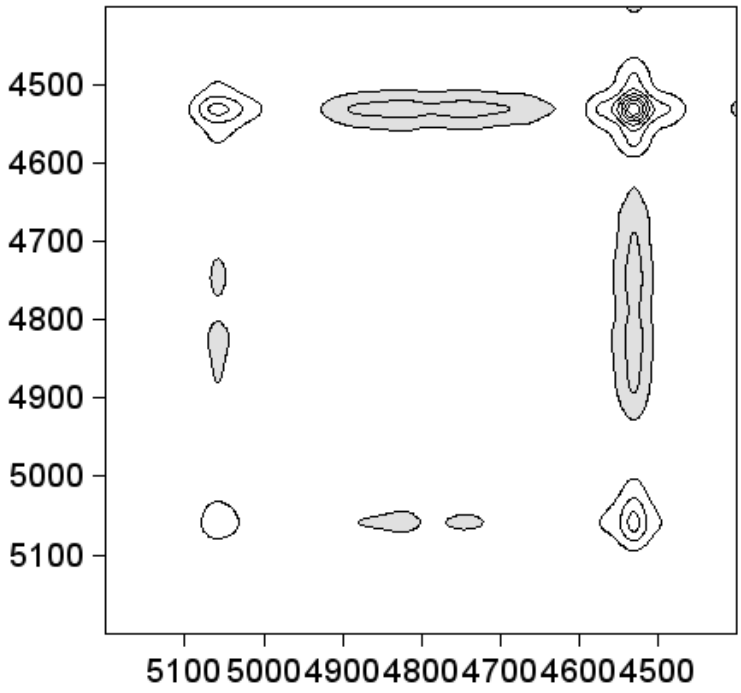

Figure 7. Synchronous map in the 5200-5400 cm^{-1} region without outlier data.

Although 2Dshige© software can process the entire data file for the spectrum, specific output ranges typically are selected when generating correlation maps to better view specific regions. In this study, the spectrum was broken into three smaller regions for analysis. The 5200-4400 cm^{-1} region was selected to look for the disappearance of the terminal epoxide ring interaction and primary amine combination band. Next, the 6200-5400 cm^{-1} region was selected for the epoxide ring C-H stretch. Finally, the 7200-6400 cm^{-1} region was chosen to show hydroxide and amine overtones. Synchronous and asynchronous maps were generated for each region. Appendix A provides detailed instructions for manipulating raw time dependent absorbance data and running the 2Dshige© program.

Reading Correlation Maps

In each map negative peaks are marked as shaded regions on a contour map or in blue colors on a color map. Likewise, positive peaks are marked without shading on a contour map or in red colors on a color map. For a synchronous map, the intensity of the shading or coloring of a peak represents the simultaneous or coincidental changes to two separate spectral variations. Peaks located on the diagonal (autopeaks) are a function of autocorrelation (i.e., the spectral change is cross-correlated with itself) and are always positive. A stronger intensity means that the band is more susceptible to the perturbation enacted on the system. Peaks located at off diagonal positions are referred to as cross-peaks*;* these may be positive or negative. A positive sign indicates that the two bands vary in the same direction, whereas a negative sign means the bands vary in opposite directions. It is customary to analyze the cross-peaks located to the left of the diagonal line.

In the asynchronous spectrum, intensities indicate sequential spectral changes. The asynchronous spectrum contains no autopeaks, only cross-peaks which develop when spectral changes are out-of-phase with each other. The sign of the cross-peak determines the sequence: a positive peak indicates that the x-coordinate band varies before the y-coordinate band. However, the sign of the related cross-peak in the synchronous spectrum must also be taken into account. If the corresponding synchronous peak is negative, then the sequence is reversed. (Noda & Ozaki, 2004) These rules, commonly called *Noda's Rules,* are shown in Table 2. Using the table,

chemical changes can be sequenced based on the signs of corresponding cross-peaks in the asynchronous and synchronous maps.

Table 2. Noda's rules.

Asynchronous Cross-peak	Synchronous Cross-peak	Sequence
Positive (γ_1,γ_2)	Positive (γ_1,γ_2)	γ_1 varies before γ_2
Positive (γ_1,γ_2)	Negative (γ_1,γ_2)	γ_1 varies after γ_2
Negative (γ_1,γ_2)	Positive (γ_1,γ_2)	γ_1 varies after γ_2
Negative (γ_1,γ_2)	Negative (γ_1,γ_2)	γ_1 varies before γ_2

Results and Discussion

2D Correlation Spectra in the 5200-4400 cm^{-1} Region

This region typically exhibits epoxide stretching interactions and disappearance of the primary amine combination band. In Fig. 8, autopeaks are observed at 5058 and 4531 cm^{-1} in the synchronous spectrum. There is also a broad autopeak between 4750-4825 cm^{-1}, centered at 4790 cm^{-1}. The peak at 5058 cm^{-1} can be attributed to a primary amine combination band. The weak-intensity, but broad, 4750-4825 cm^{-1} peak represents a hydroxyl combination band. In a study of isothermal curing of epoxy pre-preg, Wang, Storm, and Houmoller (2003) identified a NIR hydroxyl combination peak at 4795 cm^{-1}, while Li, Wu, Li, and Wu (2008) assigned the 4890-4786 cm^{-1} region to an OH combination band. The strong 4531 cm^{-1} autopeak can be attributed to epoxide ring combination band. One positive and four negative cross-peaks can be observed (Table 3) in the upper left half of map. The 5058 and 4531 cm^{-1} peaks share positive cross-peaks and thus vary in the same direction, while the 4790 cm^{-1} band moves in the opposite direction. From Fig.1, it can be determined that the epoxide and primary amine (4531 and 5058 cm^{-1} bands) decrease while the hydroxyl group (4750-4825 cm^{-1}) increases. These spectral changes are consistent with hydroxyl group formation as a result of amine consumption.

Of the cross-peaks identified on the synchronous map, two positive and three negative cross-peaks appear in the asynchronous correlation map in Fig. 9. Only the (5058, 4825 cm^{-1}) peak does not appear. Adhering to Noda's Rules, the peaks indicate that the primary amine combination band varies before hydroxyl formation, which varies before the epoxy ring combination (5058 → 4750-4825 → 4531 cm^{-1}). More specifically, the primary amine is disappearing before the epoxide ring is opened.

Table 3. Peak data for the 5200-4400 cm^{-1} region.

(ν_1,ν_2)	Synchronous	Direction	Asynchronous	Sequence
5058, 4825	NEG	↓,↑	N/A	Same
5058, 4750	NEG	↓,↑	NEG	5058→4750
5058, 4531	POS	↓,↓	POS	5058→4531
4825, 4750	POS	↑,↑	POS	4825→4750
4825, 4531	NEG	↑,↓	NEG	4825→4531
4750, 4531	NEG	↑,↓	NEG	4750→4531

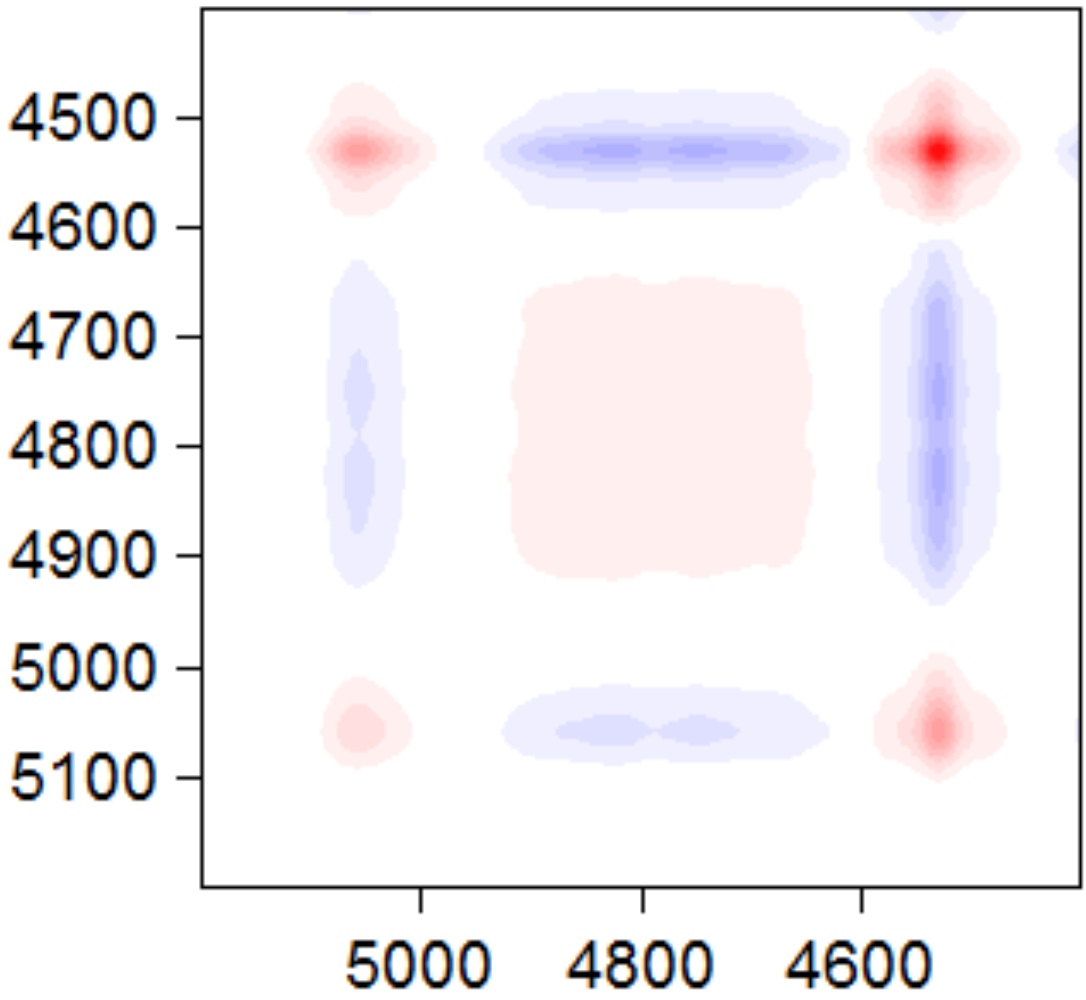

Figure 8. Synchronous correlation map for the 5200-4400 cm^{-1} region. Negative peaks are marked in blue. All axes are in cm^{-1}.

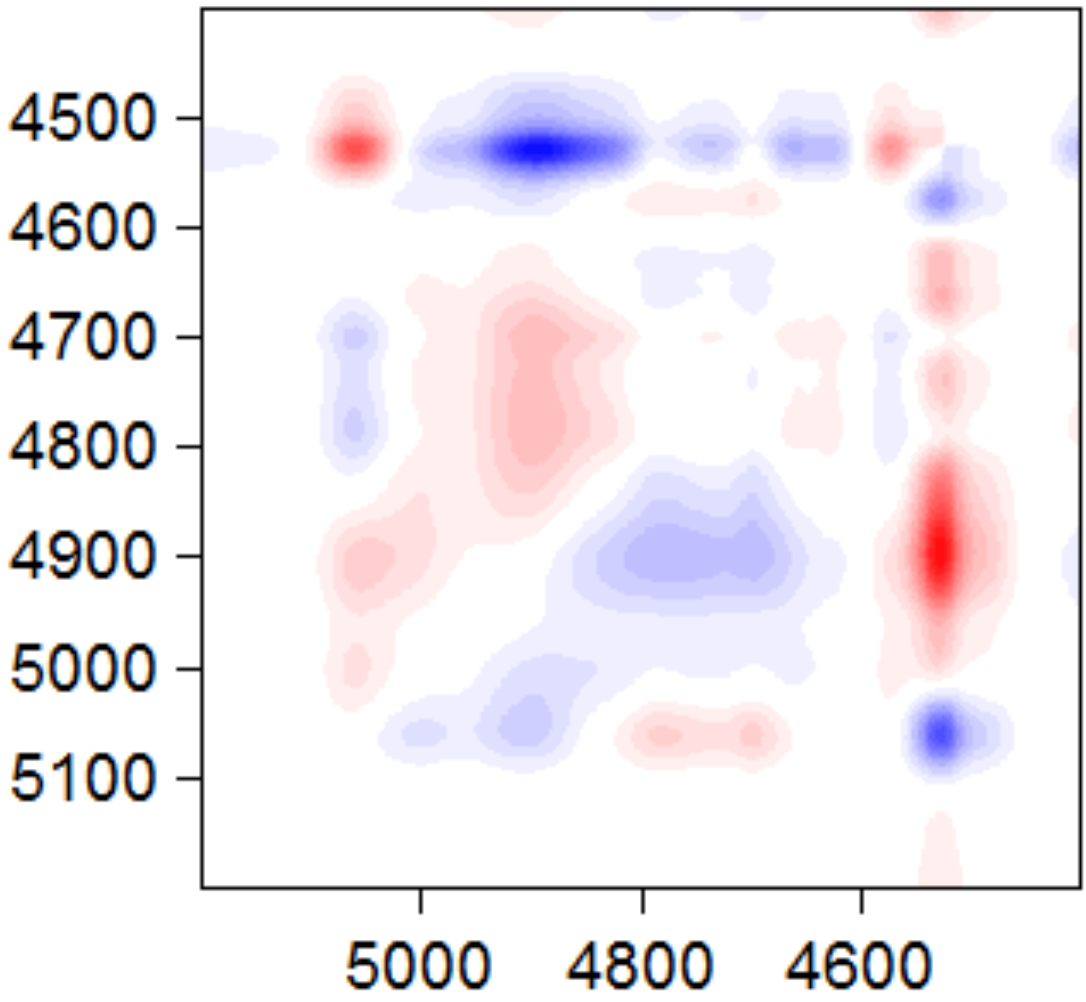

Figure 9. Asynchronous correlation map for the 5200-4400 cm^{-1} region. Negative peaks are marked in blue. All axes are in cm^{-1}.

2D Correlation Spectra in the 6200-5400 cm^{-1} Region

In this complex region the abundance of peaks are related to terminal epoxide CH_2 stretching overtones and epoxy—CH/CH_2 combination bands. In Fig. 10, six autopeaks occur at 6076, 6018, 5890, 5719, 5628, and 5542 cm^{-1} in the synchronous spectrum. The 6076 cm^{-1} peak can be attributed to terminal epoxy ring stretch. Interestingly, the 6018 cm^{-1} peak is not easily seen with standard absorbance graphs and was not previously identified by Fu and Schlup (1993). Dumitrescu, Baker, Foster, and Evans (2005) related the 6018 cm^{-1} peak to aromatic C-H stretching vibration overtones. The 5890 cm^{-1} peak can be assigned to an epoxy—CH/CH_2 combination band. The broad autopeak centered at 5628 cm^{-1} is a result of CH/CH_2 overtones and consists of several smaller overlapping peaks in the range of 5719 to 5542 cm^{-1}. As hydrogen bonds form, wavenumber positions can shift due to modifications in the molecular vibrations (Ozaki, Noda, 2005), thus creating overlapping peaks resulting in line broadening. Seven positive and eight negative cross-peaks are observed in the upper left portion of the synchronous spectrum and are listed in Table 4. From these data points, the 6076 and 5890 cm^{-1} bands are both increasing. Likewise, the 6018, 5719, 5628, and 5542 cm^{-1} bands are decreasing. Chemically speaking, the terminal epoxide ring stretch overtone and the epoxy—CH/CH_2 combination bands are increasing. The C-H stretching and CH/CH_2 vibration overtones are both decreasing.

In the corresponding asynchronous spectrum (Fig. 11), seven positive and one negative cross-peaks occur. Seven expected cross-peaks are absent from the asynchronous map because the bands vary simultaneously. Using Noda's rules, the bands vary in the sequence 6018, 5719, 5628, 5542 → 6076, 5890 cm^{-1}. C-H stretching overtones and CH/CH_2 vibration overtones decrease before the epoxy—CH/CH_2 combination band and terminal epoxide CH_2 stretching overtone increase.

Table 4. Peak data for the 6200-5400 cm^{-1} region.

(ν_1,ν_2)	Synchronous	Direction	Asynchronous	Sequence
6076, 6018	NEG	↑,↓	POS	6018→6076
6076, 5890	POS	↑,↑	N/A	Same
6076, 5719	NEG	↑,↓	POS	5719→6076
6076, 5628	NEG	↑,↓	POS	5628→6076
6076, 5542	NEG	↑,↓	POS	5542→6076
6018, 5890	NEG	↓,↑	NEG	6018→5890
6018, 5719	POS	↓,↓	N/A	Same
6018, 5628	POS	↓,↓	N/A	Same
6018, 5542	POS	↓,↓	N/A	Same
5890, 5719	NEG	↑,↓	POS	5719→5890
5890, 5628	NEG	↑,↓	POS	5628→5890
5890, 5542	NEG	↑,↓	POS	5542→5890
5719, 5628	POS	↓,↓	N/A	Same
5719, 5542	POS	↓,↓	N/A	Same
5628, 5542	POS	↓,↓	N/A	Same

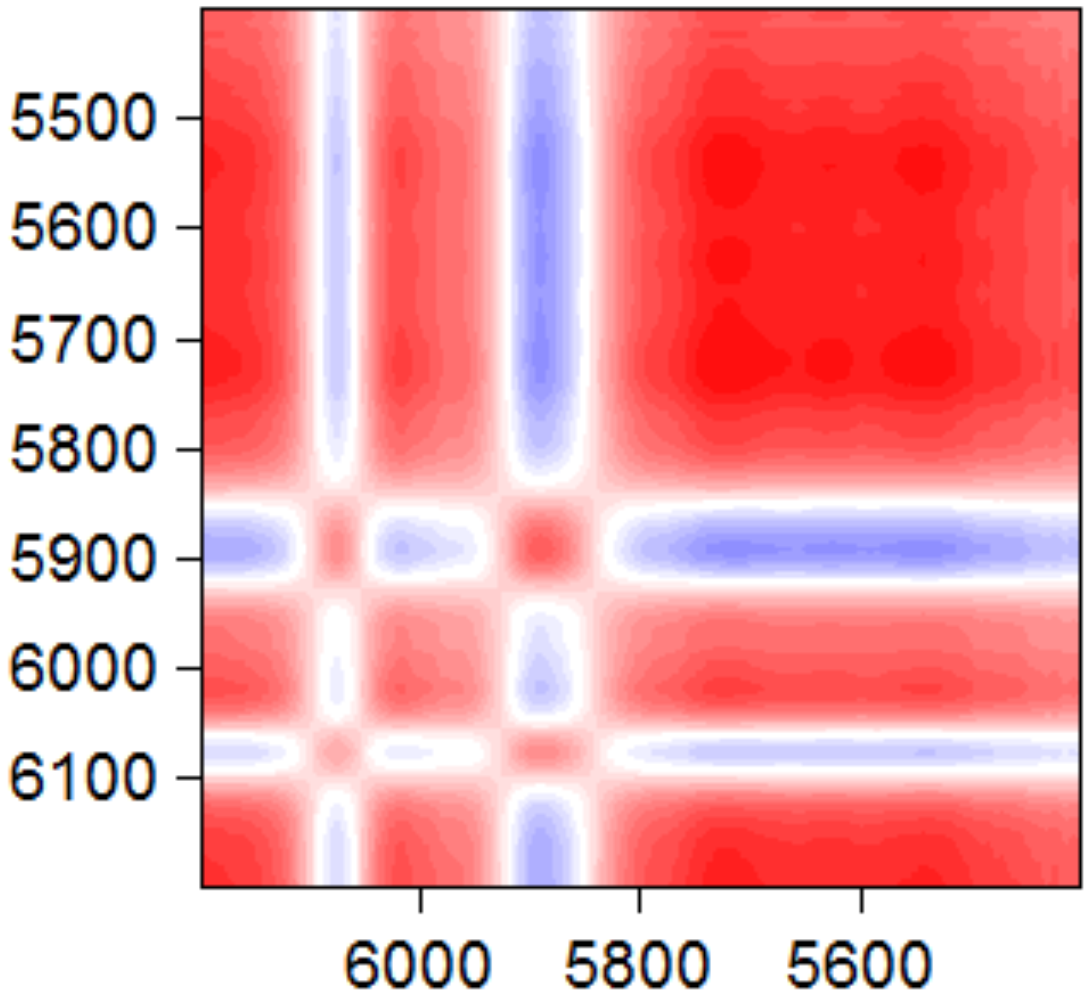

Figure 10. Synchronous correlation map for the 6200-5400 cm^{-1} region. Negative peaks are marked in blue. All axes are in cm^{-1}.

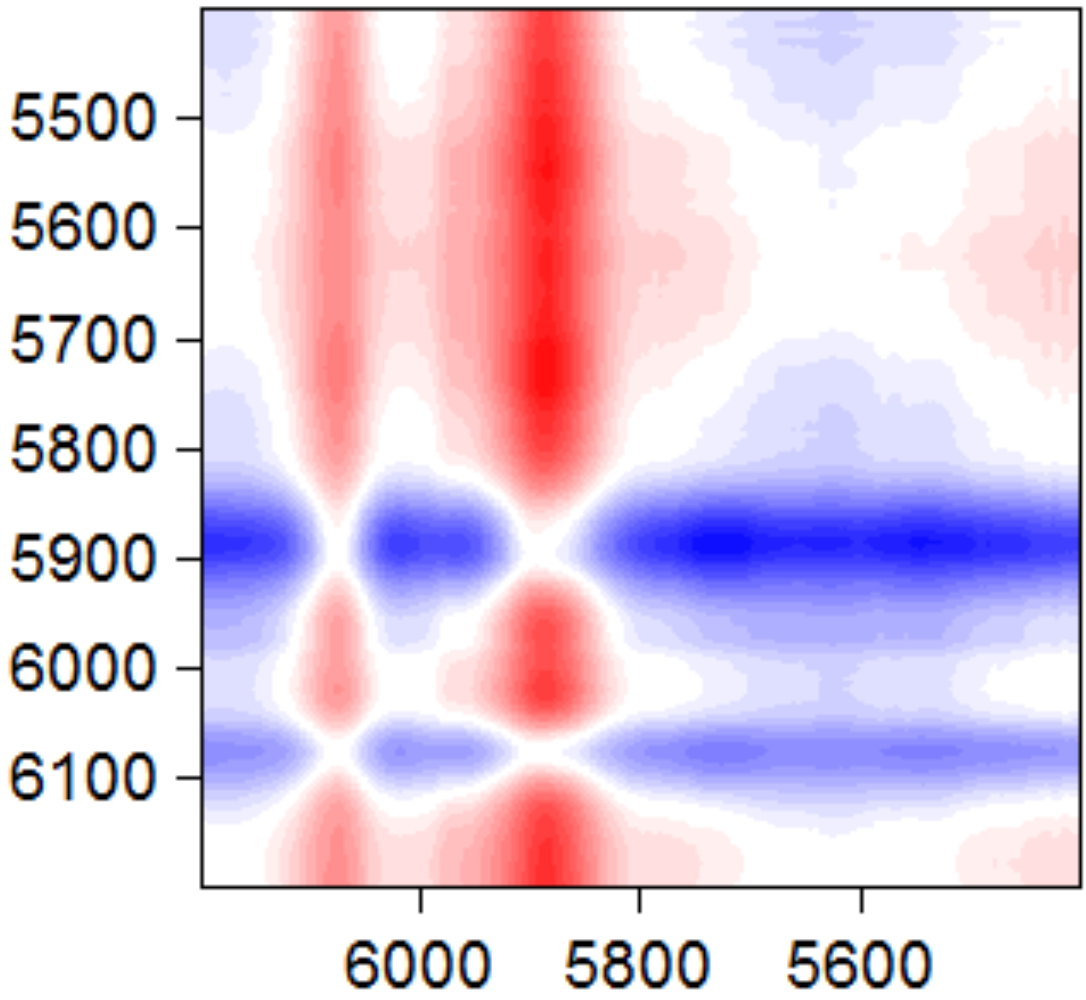

Figure 11. Asynchronous correlation map for the 6200-5400 cm^{-1} region. Negative peaks are marked in blue. All axes are in cm^{-1}.

2D Correlation Spectra in the 7200-6400 cm^{-1} Region

Since the N-H vibrational overtones appear in the 6577 to 6690 cm^{-1} range, this region should elucidate the primary and secondary amine overlap. The synchronous map in Fig. 12 exhibits a single weak intensity autopeak at 6658 cm^{-1}, which is somewhat surprising since Fu and Schlup (1993) identified the primary amine overtone and secondary amine overtone near 6652 and 6641 cm^{-1}, respectively. It would seem that 2DNIR fails to separate the overtone into two distinct peaks on the synchronous map. The intense autopeak at 6987 cm^{-1} is a result of hydroxyl overtones. Based on the negative sign of the cross-peak in the upper left half of the correlation map, the bands vary in different directions. Again from the reaction chemistry and Fig.4, the primary amine reacts yielding a hydroxyl group.

In the corresponding asynchronous spectrum, shown in Fig. 13, the (6987, 6658 cm^{-1}) peak splits into two distinct peaks located at (6987, 6624 cm^{-1}) and (6987, 6699 cm^{-1}) as shown in Table 5. These separate peaks are most likely due to the primary and secondary amine overtones. Following Noda's Rules, the peaks vary according to 6987 → 6658 cm^{-1}; the hydroxyl overtone varies before the primary amine overtone. In terms of the reaction, it appears that the epoxy ring opens prior to the amine reaction. This sequence contradicts the information from the 5200-4400 cm^{-1} region. In that region the combination band overtones indicate that the amine disappears before ring opening.

Table 5. Peak data for the 7200-6400 cm^{-1} region.

(ν_1,ν_2)	Synchronous	Direction	Asynchronous	Sequence
6987, 6658	NEG	↑,↓	NEG	6987→6658
6987, 6624	N/A	↑,↓	NEG	6987→6624
6987, 6699	N/A	↑,↓	NEG	6987→6699

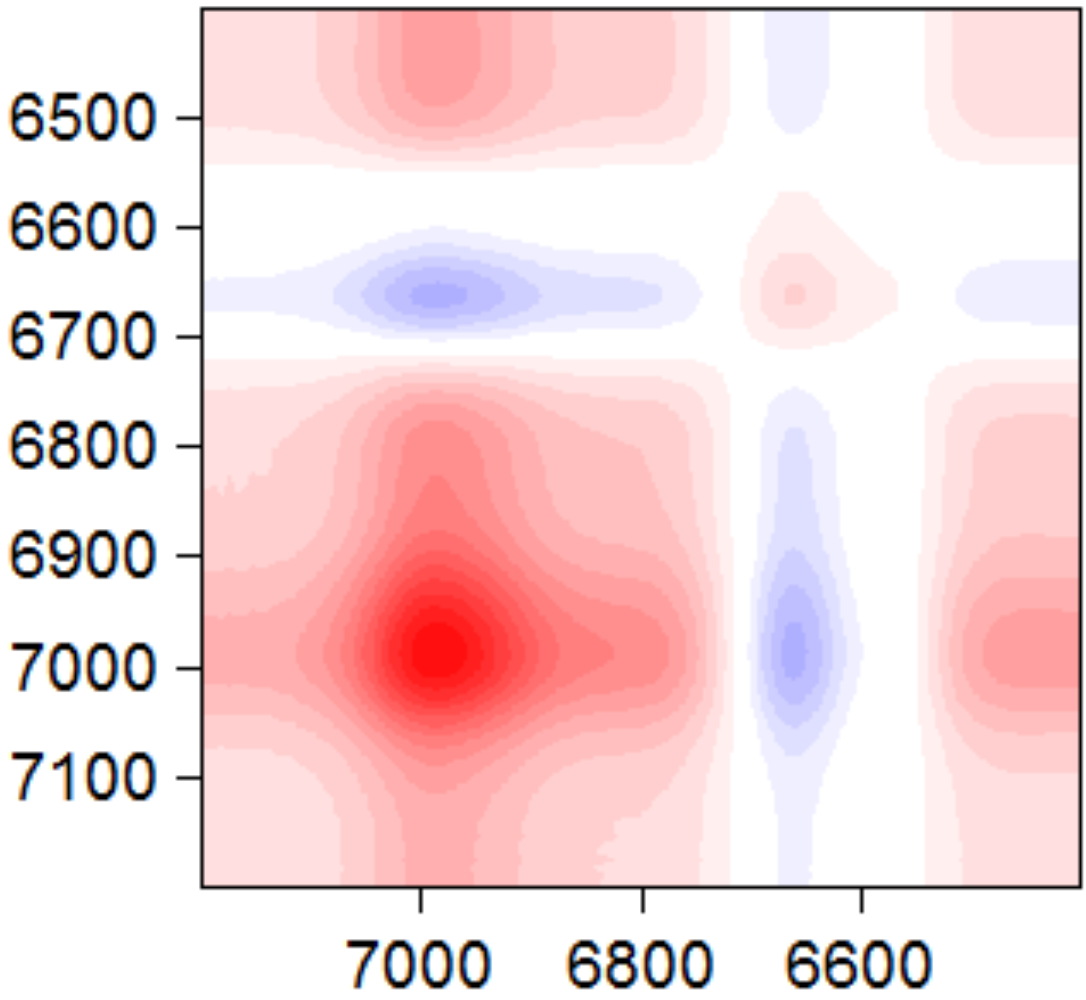

Figure 12. Synchronous correlation map for the 7200-6400 cm^{-1} region. Negative peaks are marked in blue. All axes are in cm^{-1}.

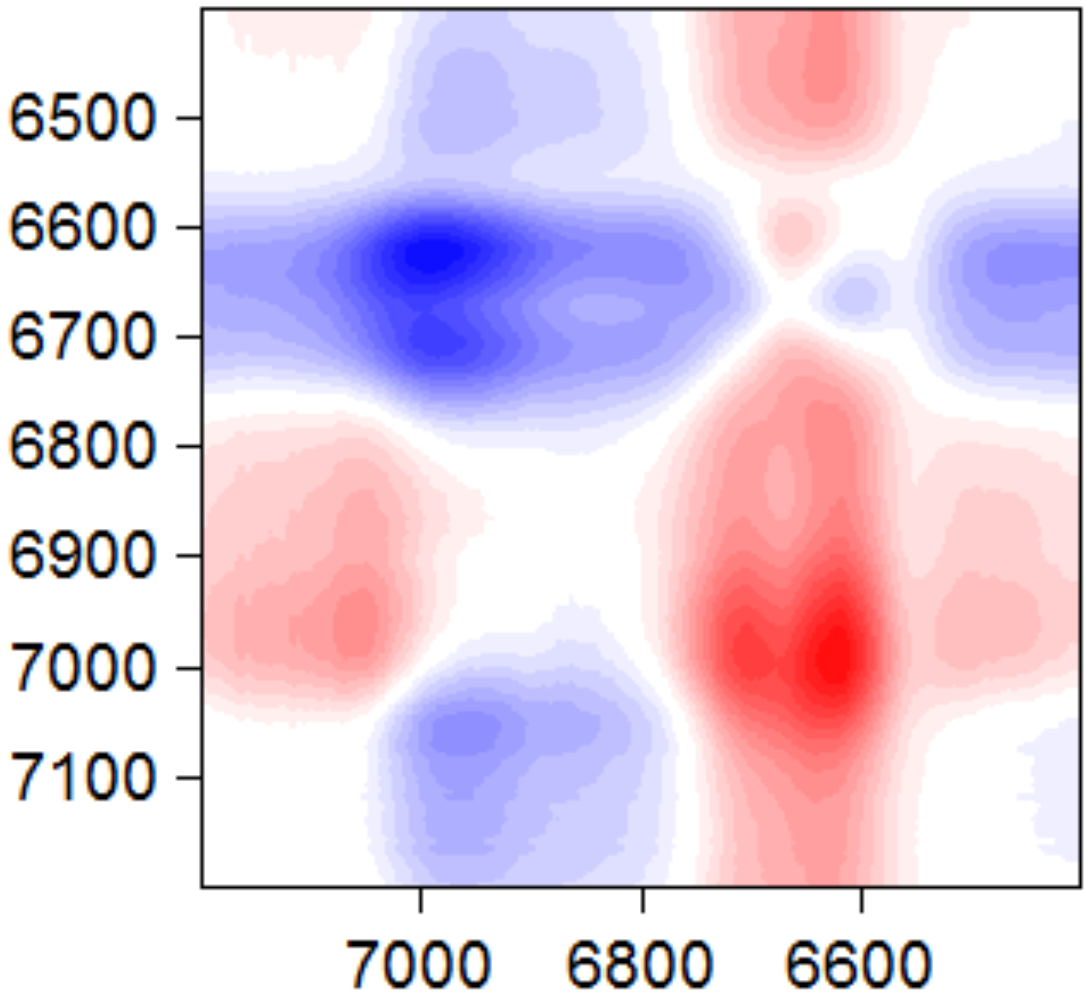

Figure 13. Asynchronous correlation map for the 7200-6400 cm^{-1} region. Negative peaks are marked in blue. All axes are in cm^{-1}.

Finally, Table 6 summarizes the tentative assignments of the characteristic peaks for the system identified in this paper.

Table 6. Characteristic peaks for mPDA/PGE.

Position (cm^{-1})	Assignment	Direction
4531	Epoxide ring combination	Decreasing
4750, 4825	Hydroxyl combination	Increasing
5058	Primary amine combination	Decreasing
5719, 5628, 5542	CH/CH_2 overtones	Decreasing
5890	Epoxy-CH/CH_2 combination	Increasing
6018	C-H stretching vibration overtone	Decreasing
6076	Terminal epoxide ring stretch overtone	Increasing
6658	Primary amine overtone	Decreasing
6987	Hydroxyl overtone	Increasing

2D Correlation Spectra Regions Compared

Since the data was broken down into smaller regions for clarity, these regions can be compared against one another by altering the axes on the correlation maps in 2Dshige©. Comparing regions can better help sequence all of the spectral changes.

7200-6400 cm^{-1} vs. 6200-5400 cm^{-1} Region

In comparing these regions, the synchronous spectrum (Fig. 14) exhibits six positive and six negative peaks. The direction (positive or negative) of each band indicates that the hydroxyl overtone (6987 cm^{-1}), C-H stretching vibration overtone (6018 cm^{-1}), and the CH/CH_2 overtones (5719, 5628, 5542 cm^{-1}) all vary in one direction while the primary amine overtone (6658 cm^{-1}), terminal epoxy ring stretch overtone (6076 cm^{-1}), and epoxy—CH/CH2 combination (5890 cm^{-1}) vary together in the opposite direction.

Many of the cross-peaks seen in the synchronous map are not present in the asynchronous map. This phenomenon occurs when two bands vary simultaneously. As a result the asynchronous spectrum (Fig. 15) exhibits four positive and two negative peaks. Missing are the cross-peaks for (6987, 6018 cm^{-1}), (6987, 5719 cm^{-1}), (6987, 5628 cm^{-1}), (6987, 5542 cm^{-1}), (6658, 6076 cm^{-1}), and (6658, 5890 cm^{-1}). According to Noda's Rules, these cross- peaks indicate that the sequence occurs in the following manner: 6987/6018/5719-5542 → 6658/6076 → 5890 cm^{-1}. This sequence indicates that the appearance of the OH groups and CH backbone vibrations occurs before the primary amine reactions and epoxide ring opening. The findings here contradict those found by Li, Wu, Li & Wu (2008) in a DGEBA/DDM system in which the 2DNIR data suggested that the NH_2 and epoxy groups changed first, followed by the OH groups and CH/CH_2 of the backbone.

Table 7. Peak data for the 7200-6400 vs. 6200-5400 cm^{-1} region.

(ν_1,ν_2)	Synchronous	Direction	Asynchronous	Sequence
6987, 6076	NEG	↑,↓	NEG	6987→6076
6987, 6018	POS	↑,↑	N/A	Same
6987, 5890	NEG	↑,↓	NEG	6987→5890
6987, 5719	POS	↑,↑	N/A	Same
6987, 5628	POS	↑,↑	N/A	Same
6987, 5542	POS	↑,↑	N/A	Same
6658, 6076	POS	↓,↓	N/A	Same
6658, 6018	NEG	↓,↑	POS	6018→6658
6658, 5890	POS	↓,↓	N/A	Same
6658, 5719	NEG	↓,↑	POS	5719→6658
6658, 5628	NEG	↓,↑	POS	5628→6658
6658, 5542	NEG	↓,↑	POS	5542→6658

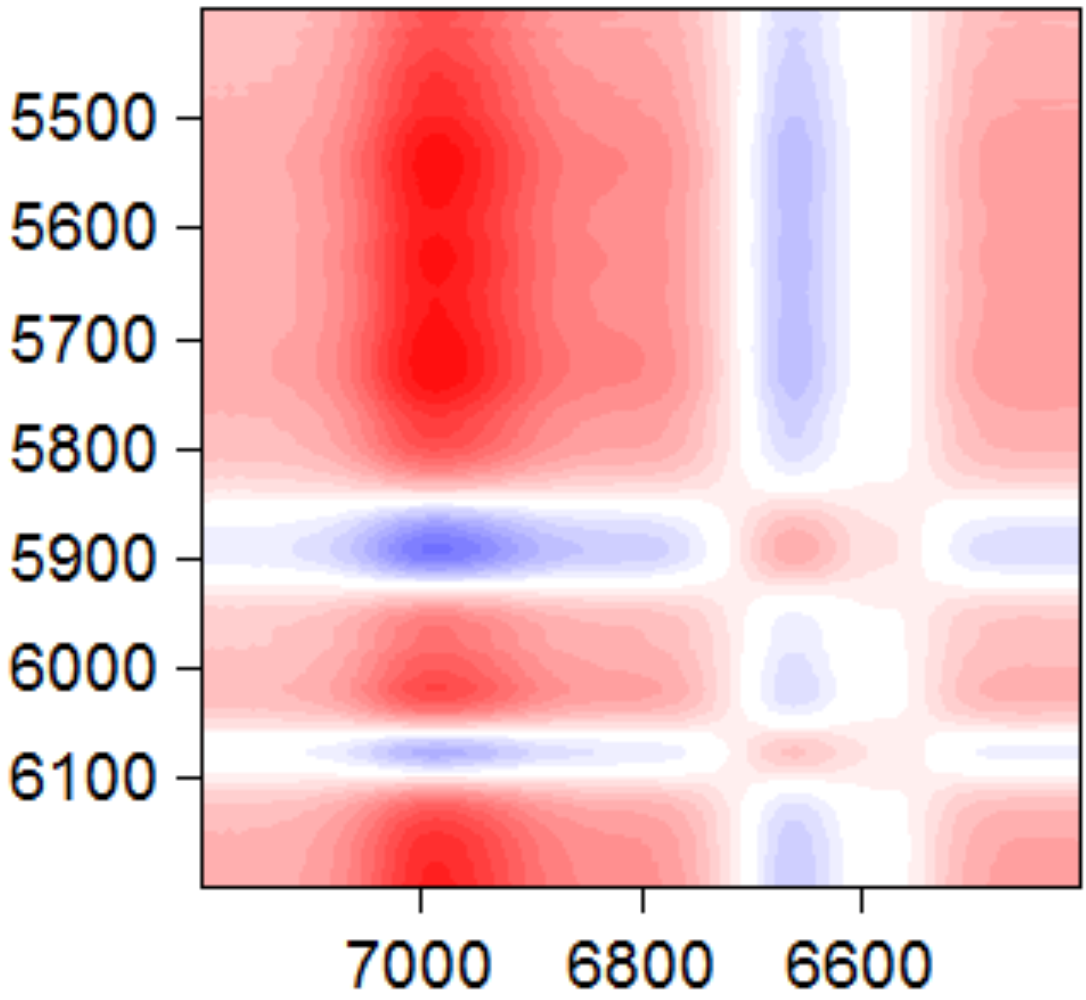

Figure 14. Synchronous correlation map for the 7200-6400 vs. 6200-5400 cm^{-1} region. Negative peaks are marked in blue. All axes are in cm^{-1}.

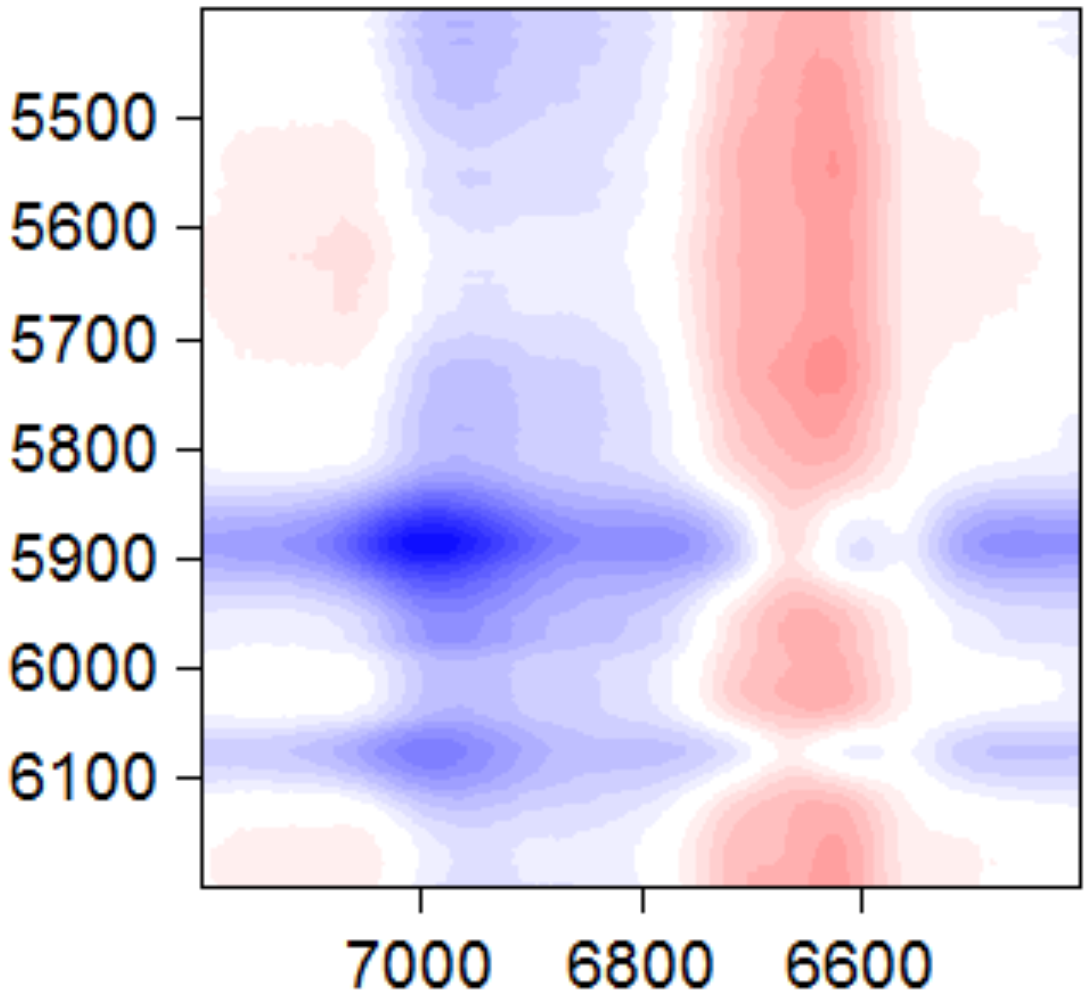

Figure 15. Asynchronous correlation map for the 7200-6400 vs. 6200-5400 cm^{-1} region. Negative peaks are marked in blue. All axes are in cm^{-1}.

7200-6400 cm^{-1} vs. 5200-4400 cm^{-1} Region

Four positive and four negative peaks appear in the entire synchronous map (Fig. 16) for this region and are listed in Table 8. The signs on the map indicate that the hydroxyl overtone (6987 cm^{-1}) and hydroxyl combination bands (4825-4750 cm^{-1}) are increasing while the primary amine overtone (6658 cm^{-1}), primary amine combination (5058 cm^{-1}), and epoxy ring combination (4531 cm^{-1}) are decreasing.

Of the eight cross-peaks seen in the synchronous map, only one positive cross- peak (6987, 5058 cm^{-1}) and two negative cross-peaks [(6987, 4531 cm^{-1}) and (6658, 5058 cm^{-1})] appear on the asynchronous map in Fig. 17. The other corresponding points may fall into a positive or negative area, but no peak exists at the specific point. By comparing the signs of the peaks in these two regions, the following sequence can be derived: 6987/4825/4790 → 6658/5058/4531 cm^{-1}. This sequence indicates an increase in OH groups before the disappearance of the amines. Data from Li, Wu, Li & Wu (2008) suggested the opposite sequence: the NH_2 groups changed prior to the OH groups.

Table 8. Peak data for the 7200-6400 vs. 5200-4400 cm^{-1} region.

(ν_1,ν_2)	Synchronous	Direction	Asynchronous	Sequence
6987, 5058	NEG	↑,↓	POS	6987→5058
6987, 4825	POS	↑,↑	N/A	Same
6987, 4750	POS	↑,↑	N/A	Same
6987, 4531	NEG	↑,↓	NEG	6987→4531
6658, 5058	POS	↓,↓	NEG	5058→6658
6658, 4825	NEG	↓,↑	N/A	Same
6658, 4750	NEG	↓,↑	N/A	Same
6658, 4531	POS	↓,↓	N/A	Same

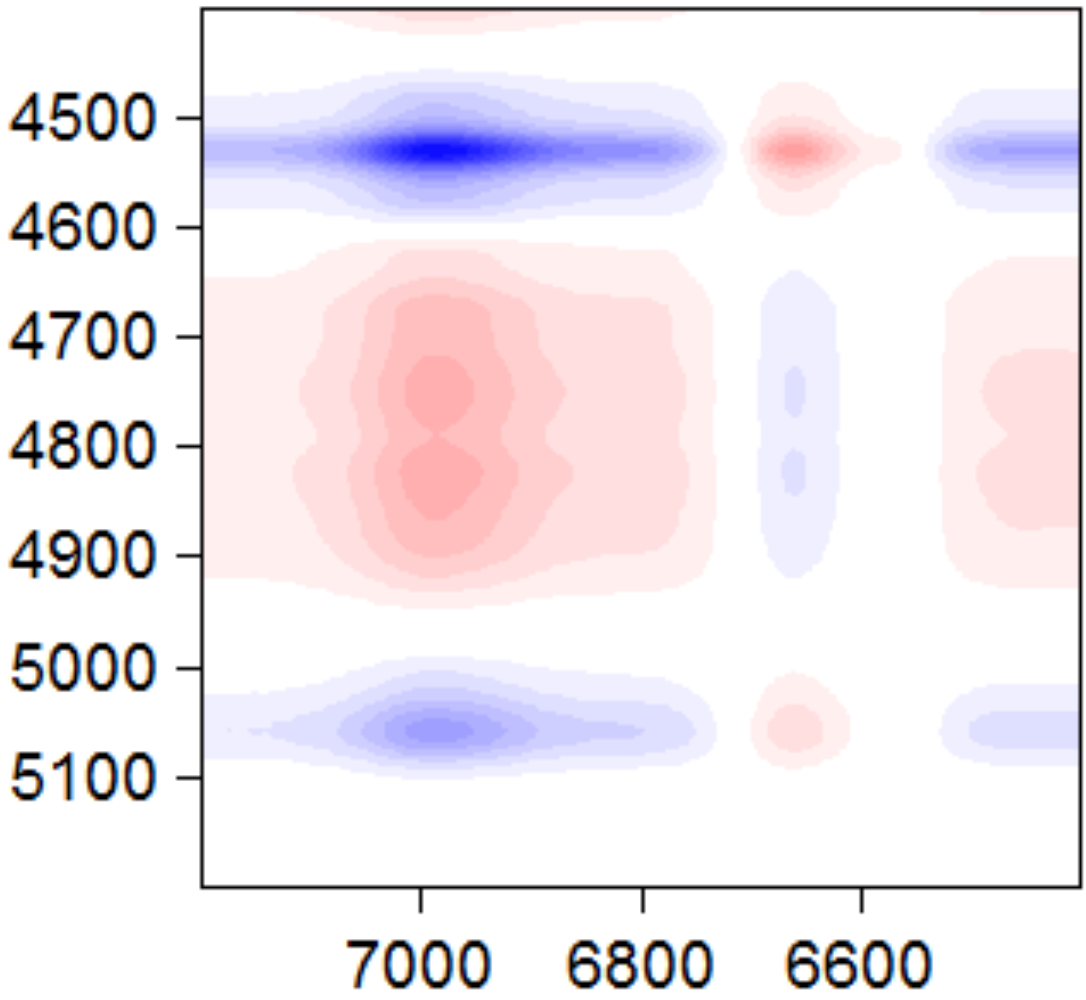

Figure 16. Synchronous correlation map for the 7200-6400 vs. 5200-4400 cm^{-1} region. Negative peaks are marked in blue. All axes are in cm^{-1}.

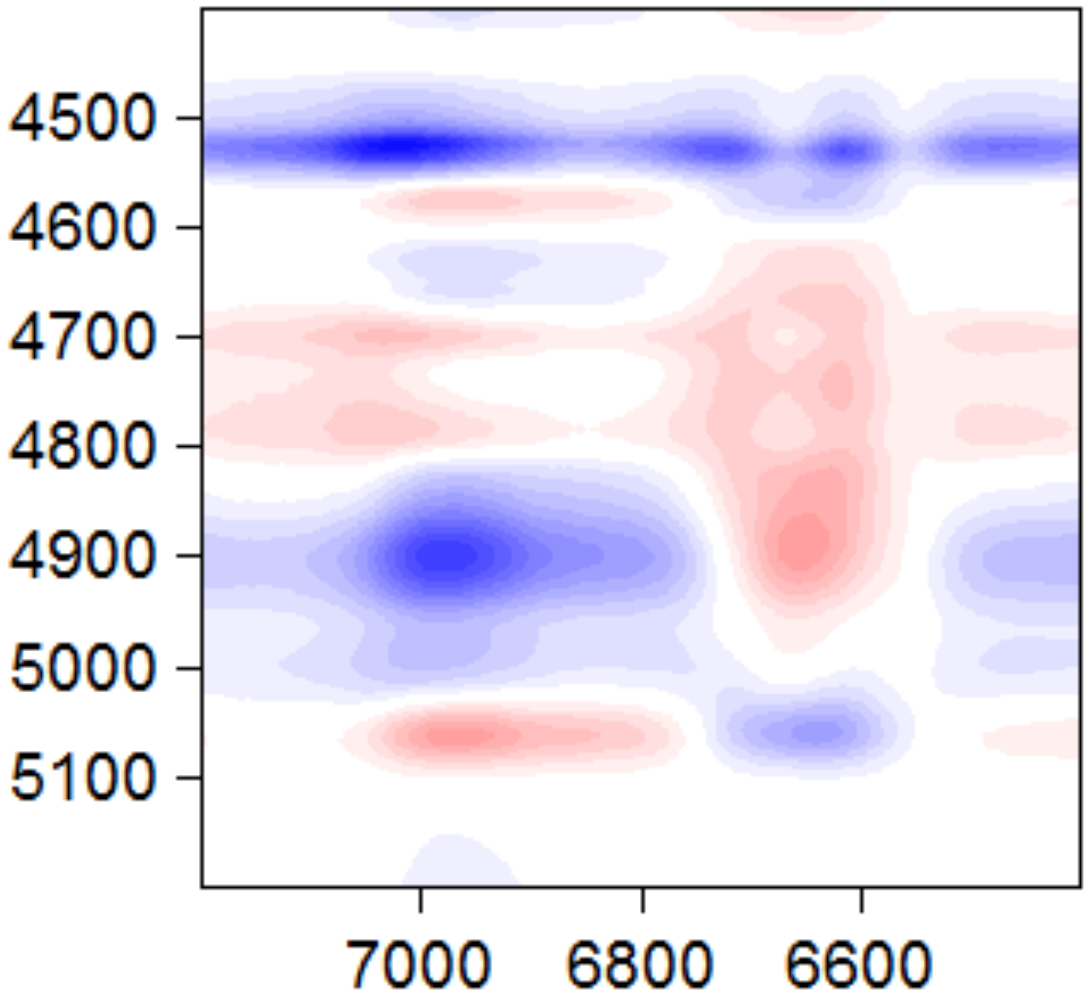

Figure 17. Asynchronous correlation map for the 7200-6400 vs. 5200-4400 cm^{-1} region. Negative peaks are marked in blue. All axes are in cm^{-1}.

6200-5400 cm^{-1} vs. 5200-4400 cm^{-1} Region

In this comparison, the synchronous map (Fig. 18) exhibits 12 positive and 12 negative peaks over the whole map. Of the 24 corresponding cross-peaks found on the synchronous map, only seven positive peaks and six negative peaks are present on the asynchronous map in Fig.19.

From the peak data listed in Table 9, the sequence of changes in the reaction occurs in the following manner: 5058 → 6018/5719/5628/5542 → 4825/4750 → 4531 → 6076/5890 cm^{-1}. The sequence suggests that the NH_2 groups decrease, followed by increases in the C-H stretching vibration, CH/CH2 overtones, and hydroxyl groups, then a decrease in the terminal epoxy ring overtone, ring stretch, and epoxy-CH/CH_2 combination.

Table 9. Peak data for the 6200-5400 vs. 5200-4400 cm^{-1} region.

(ν_1,ν_2)	Synchronous	Direction	Asynchronous	Sequence
6076, 5058	POS	↑,↑	NEG	5058→6076
6076, 4825	NEG	↑,↓	N/A	Same
6076, 4750	NEG	↑,↓	POS	4750→6076
6076, 4531	POS	↑,↑	N/A	Same
6018, 5058	NEG	↓,↑	POS	5058→6018
6018, 4825	POS	↓,↓	N/A	Same
6018, 4750	POS	↓,↓	POS	6018→4750
6018, 4531	NEG	↓,↑	NEG	6018→4531
5890, 5058	POS	↑,↑	NEG	5058→5890
5890, 4825	NEG	↑,↓	N/A	Same
5890, 4750	NEG	↑,↓	POS	4750→5890
5890, 4531	POS	↑,↑	NEG	4531→5890
5719, 5058	NEG	↓,↑	N/A	Same
5719, 4825	POS	↓,↓	N/A	Same
5719, 4750	POS	↓,↓	N/A	Same
5719, 4531	NEG	↓,↑	NEG	5719→4531
5628, 5058	NEG	↓,↑	POS	5058→5628
5628, 4825	POS	↓,↓	N/A	Same
5628, 4750	POS	↓,↓	POS	5628→4750
5628, 4531	NEG	↓,↑	N/A	Same
5542, 5058	NEG	↓,↑	N/A	Same
5542, 4825	POS	↓,↓	N/A	Same
5542, 4750	POS	↓,↓	POS	5542→4750
5542, 4531	NEG	↓,↑	NEG	5542→4531

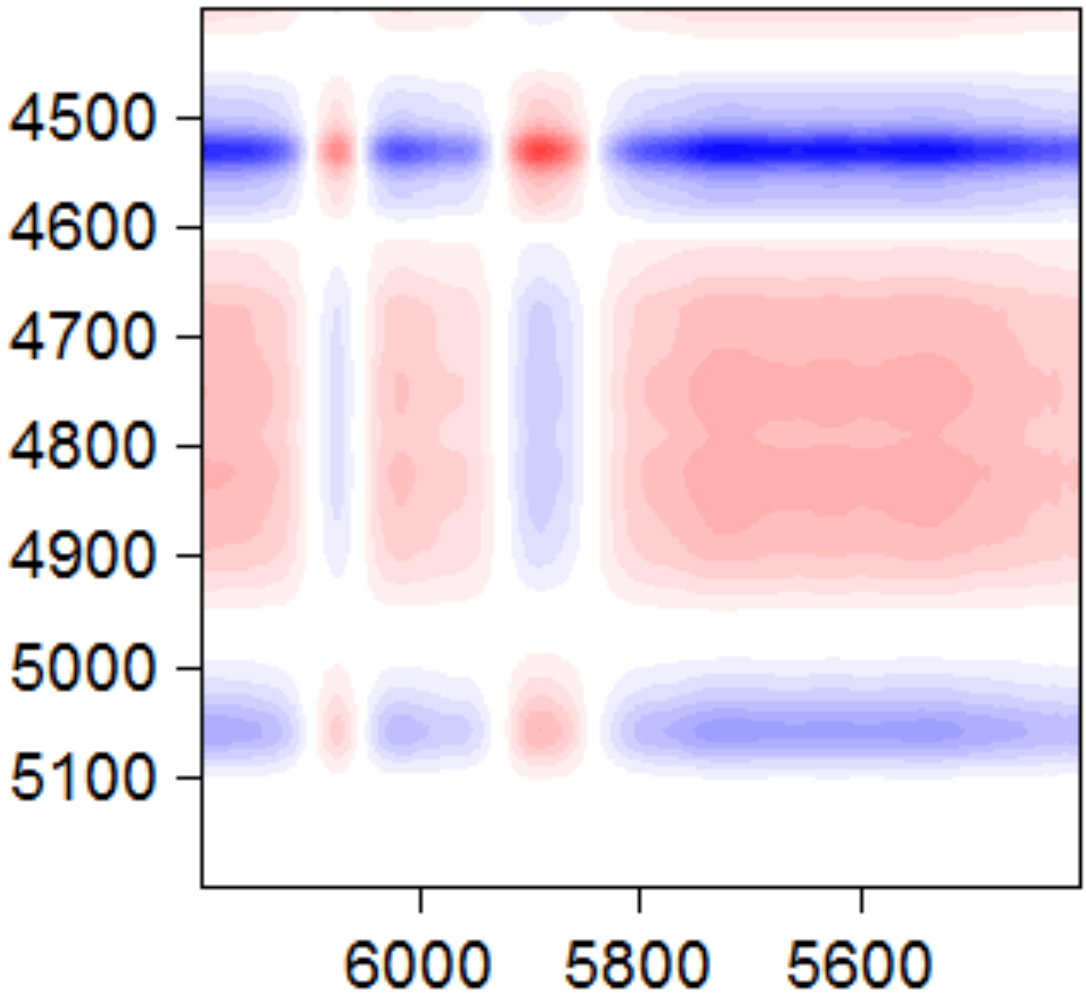

Figure 18. Synchronous correlation map for the 6200-5400 vs. 5200-4400 cm^{-1} region. Negative peaks are marked in blue. All axes are in cm^{-1}.

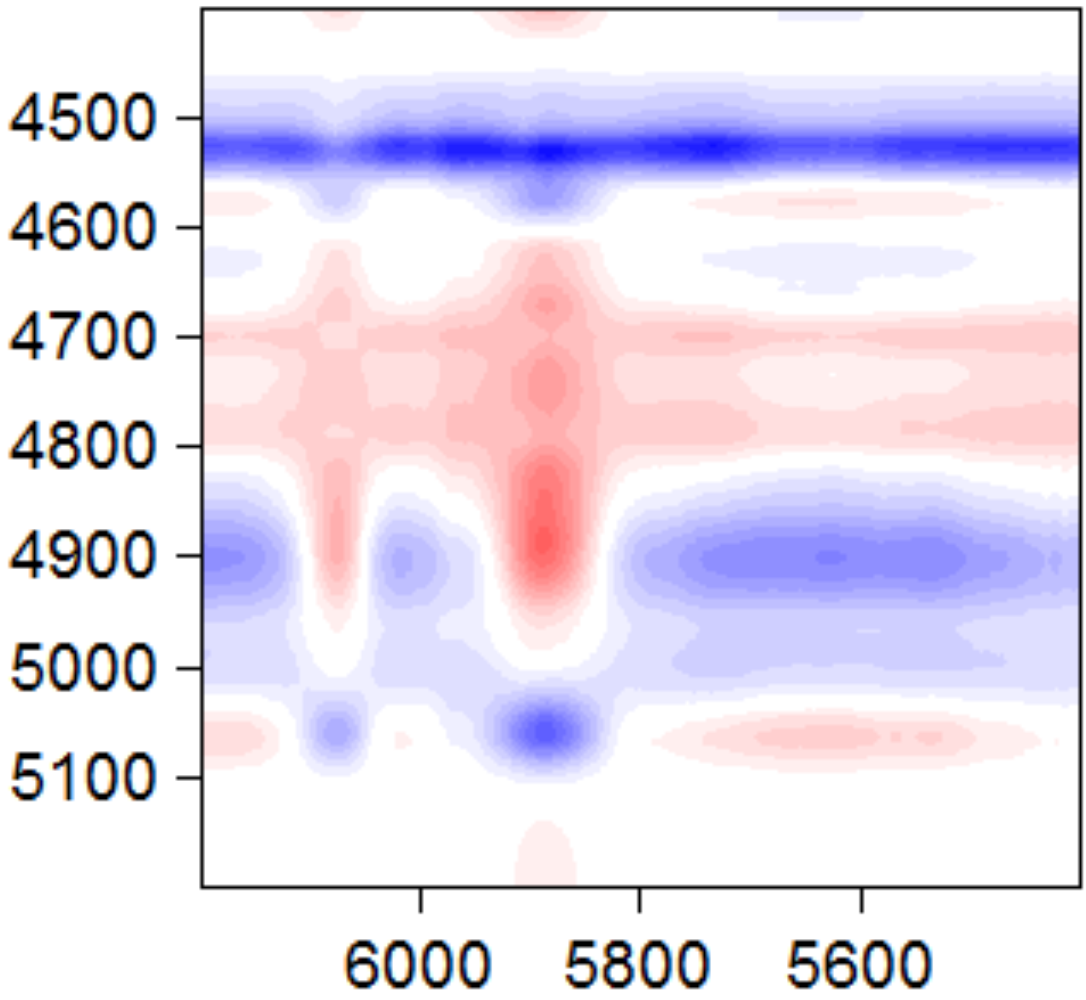

Figure 19. Asynchronous correlation map for the 6200-5400 vs. 5200-4400 cm^{-1} region. Negative peaks are marked in blue. All axes are in cm^{-1}.

Conclusion

In summary, 2Dshige© was debugged and applied to the NIR data set for the PGE/mPDA system. Correlation maps showed the peaks previously identified by Fu & Schlup (1993) and even identified new peaks for the O-H combination band in the 4825-4750 cm^{-1} region and the C-H stretching vibration overtone at 6018 cm^{-1}. However, 2DNIR failed to separate the previously identified primary and secondary amine overtones at 6652 and 6641 cm^{-1}, respectively. The application of Noda's rules to 2DNIR maps also allowed for the sequencing of events, albeit with some contradiction with respect to the OH groups. In spite of the few shortcomings, 2DNIR proved a useful tool for this system. The application of 2D hetero-spectral correlation (combining two separate measurements via a common theme) using 2DNIR and NMR or ultrasonic spectroscopy would yield even more information about this system.

Bibliography

Aggelis, D., & Paipetis, A. (2012). Monitoring of resin curing and hardening by ultrasound. *Construction and Building Materials , 26*, 755-760.

Amari, T., & Ozaki, Y. (2002). *Macromolecules , 35*, 8020.

Barral, L., Cano, J., Lopez, J., Lopez-Bueno, I., Nogueira, P., Torres, A., et al. (2000). Cure kinetics of amine-cured diglycidyl ether of bisphenol: A epoxy blended with poly(ether imide). *Thermochimica Acta , 344* (1-2), 127-136.

Cakic, S., Ristic, I., Jaso, V., Radicevic, R., Ilic, O., & Simendic, J. (2012). Investigation of the curing kinetics of alkyd–melamine–epoxy resin system. *Process in Organic Coatings , 73*, 415-424.

Dumitrescu, O., Baker, D., Foster, G., & Evans, K. (2005). *Polymer Testing , 24* (3), 367.

Farquharson, S., Smith, W., & Shaw, M. (2002). Correlations between molecular (Raman) and macroscopic (Rheology) data for process monitoring of thermoset composite. *JPAC(sm) Process Analytical Chemistry* , 45-53.

Fu, J. H., & Schlup, J. R. (1993). *J. Appl. Polyme Sci* , 219.

Gallot-lavallee, O., Teyssedre, G., Laurent, C., & Rowe, S. (2005). Identification of photoluminescence features of an epoxy resin based on components features and curing effects. *Polymer , 46*, 2722-2731.

Garcia, F. L. (2010). Influence of Chemical Structure of Hardener on Mechanical and Adhesive Properties of Epoxy Polymers. *Journal of Applied Polymer Science , 117* (4).

Karkanas, P., & Partridge, I. (1996). Modeling the cure of a commercial epoxy resin for application in transfer moulding. *Polymer International* , 183-191.

Kortaberria, G., Arruti, P., Gabilondo, N., & Mondragon, I. (2004). Curing of an epoxy resin modified with poly(methylmethacrylate) monitored by simultaneous dielectric/near infrared spectroscopies. *European Polymer Journal , 40*, 129-136.

Lettieri, M., & Frigione, M. (2005). FT-IR Spectroscopy Applied To The Study Of The Curing Process Of Epoxy-Amine Systems: A Literature Review . In G. Ziakov, Y. Monakov, & A. Jimenez, *Trends in Molecular and High Molecular Science* (pp. 87-102). New York: Nova Science Publishers.

Li, L., Wu, Q., Li, S., & Wu, P. (2008). *Appl. Spectroscopy , 62*, 1129.

Liu, Y. C. (2000). Two-Dimensional Visible/Near-Infrared Correlation Spectroscopy Study of Thermal Treatment of Chicken Meats. *J. Agric. Food Chem. , 48* (3), 901-908.

Merad, L., Cochez, M., Margueron, S., Jauchem, F., Ferriol, M., Benyoucef, B., et al. (2009). In-situ monitoring of the curing of epoxy resins by Raman spectroscopy. *Polymer Testing , 28*, 42-45.

Mijovic, J., & Andelic, S. (1995). *Macromolecules , 28* (8), 2787.

Min, B. G., Stachurski, Z. H., Hodgkin, J. H., & Heath, G. R. (1993). *Polymer , 34*.

Morita, S. (2004). Kwansei-Gakuin University.

Musto, P., Mascia, L., Ragosta, G., Scarinzi, G., & Villano, P. (2000). The transport of water in a tetrafunctional epoxy resin by near-infrared Fourier transform spectroscopy. *41* (2), 565-574.

Noda, I. (1993). *Applied Spectroscopy , 47*, 550.

Noda, I., & Ozaki, Y. (2004). *Two-dimentional Correlation Spectroscopy - Applications in Vibrational and Optical Spectroscopy.* West Sussex, England: Wiley.

Noda, I., Dowrey, A. E., Marcott, C., Story, G. M., & Ozaki, Y. (2000). *Applied Spectroscopy , 54*, 236A.

Pazderka, T. K. (n.d.). *2D Correlation Spectroscopy and its Application in Vibrational Spectroscopy using MATLAB.* Retrieved May 16, 2012, from Institute of Chemical Technology, Prague, Department of Computing and Control Engineering: http://dsp.vscht.cz/konference_matlab/MATLAB08/prispevky/081_pazderka.pdf

Pham, H. a. (2005). Epoxy Resins. In *Ullmann's Encyclopedia of Industrial Chemistry.* Wiley-VCH.

St. John, N. A., & George, G. A. (1992). *Polymer , 33*, 2678.

Swier, S., Assche, G., & Mele, B. (2004). Reaction kinetics modeling and thermal properties of epoxy-amines as measured by modulated temperature DSC.I. linear step-growth polymerization of DGEBA-Aniline. *J. Appl. Poly. Sci , 91*, 2798-2813.

Vargas, M., Sachsenheimer, K., & Guthausen, G. (2012). In-situ investigations of the curing of a polyester resin. *Polymer Testing , 31* (1), 127-135.

Wang, Q., Storm, B., & Houmoller, L. (2003). *J. Appl. Polym Sci , 87*, 2295-2305.

Xu, L., & Schlup, J. R. (1997). *J. Appl. Polymer Sci. , 67*, 895.

Xu, L., Fu, J. H., & Schlup, J. R. (1994). *J. Am. Chem. Soc. , 116*, 2821.

Xu, L., Fu, J. H., & Schlup, J. R. (1996). *Ind. Eng. Chem. Res. , 35*, 963.

Appendix A - 2Dshige© User Notes

This appendix provides a step-by-step procedure for generating correlation maps using 2Dshige© software. The software is free for personal use and available from:

http://sci-tech.ksc.kwansei.ac.jp/~ozaki/2D-shige.htm

Liu (2000) generated 2D correlation maps using the KG2D correlation program (School of Science, Kwansei-Gakuin University, Nishinomiya, Japan) installed into Grams/32 software (Galactic Industrious Corp., Salem, NH). Additionally, correlation maps can be generated using MATLAB (Pazderka).

The original NIR absorbance data for PGE and mPDA obtained from Fu & Schlup (1993) existed in 21 separate files. All of the data was combined into a single Excel spreadsheet (large!) for manipulation. A quick plot of all the data shows a significant shift for the 2 and 12 minute data. Additionally, all data for the 3854.419, 3856.348, and 3858.276 cm^{-1} bands have infinite absorbance readings. It becomes quite apparent that any attempt at normalizing the data will be impacted by this outlying data. Correlation maps will exhibit false peaks and artificial contour lines since the program thinks that it is an actual perturbation. Therefore, a decision was made to omit all of the 0, 2 and 12 min data. The 0 min data were omitted solely to make the integration easier in Excel by having a consistent Δt. Finally, absorbance data for the three bands at 3854.419, 3856.348, and 3858.276 cm^{-1} were omitted because the instruments erroneously collected infinite absorbance readings (value of 8) at those wavenumberss. The data were then scaled back to within the 3800 to 8000 cm^{-1} range.

Calculating the Reference Spectrum

Although the manual for 2Dshige© indicates the software can analyze raw data, the program did not generate usable correlation maps with raw absorbance data. As a result, a dynamic spectrum was created by normalizing the data with a reference spectrum. The reference spectrum can simply be the ground state of the system ($T_{ref}=T_0$), the beginning data ($T_{ref}=T_{min}$),

the end of the data (T_{ref}=T_{max} or T_{ref} =T∞), or some other state. However, Noda and Ozaki (2004) recommend using the following:

$$\bar{y}(v) = \frac{1}{T_{max} - T_{min}} \int_{T_{min}}^{T_{max}} y(v,t)dt$$

This customary reference spectrum significantly cleaned up the data for use in 2Dshige© and generated much better looking correlation maps compared to the other reference spectra listed. It is suspected that most researchers are using this method.

On the same "Raw Data" tab, a new column was entered after the 192 min column to calculate the integral in the reference spectrum using Simpson's Rule. Since there needs to be even number of intervals, the 192 min data was not used. Here is the Excel formula in that column:

$$"Integral" = \frac{h}{3}[y(v,22) + 4 * y(v,32) + 2 * y(v,42) + \cdots + 4 * y(v,172) + y(v,182)]$$

Where $h = \frac{b-a}{n} = \frac{182-22}{16} = 10$

$$y(3810.059) = \frac{10}{3}(1.011 + 4 * 1.150 + 2 * 1.090 + \cdots + 4 * 1.166 + 1.013) = 160.330$$

Here's the exact formula from Excel:

Integral=h/3*(E4+4*F4+2*G4+4*H4+2*I4+4*J4+2*K4+4*L4+2*M4+4*N4+2*O4+4*P4+2*Q4+4*R4+2*S4+4*T4+U4)

The equation was then completed in another column:

$$\text{RefSpec} = \frac{1}{T_{max} - T_{min}} * Integral$$

$$\bar{y}(3810.059) = \frac{1}{182 - 182} * 160.330 = 1.002$$

Calculating the Dynamic Spectrum

Now that the reference spectrum is calculated, the dynamic spectrum is easily obtained from:

$$\tilde{y}(v) = y(v, t) - \bar{y}(v)$$

$$\tilde{y}(3810.059) = 1.011 - 1.002 = 0.009$$

Values were calculated on a new tab, "Dynamic Spectrum" using following formula:

='Raw data'!E4-'Raw data'!$X4

Creating the CSV File

2Dshige© is very finicky about CSV data files. Formulas, formatting, heading titles, multiple worksheets, etc. all cause errors with the program. All of the dynamic spectrum data were copied into a new file, and it was saved as a CSV file. Be sure that the A1 cell is blank. Wavenumbers should be in the first column starting at cell A2. Collection times should be in the top row starting at cell B1. Corresponding absorption data will populate the rest of the cell.

Running 2Dshige©

2Dshige© is Windows-based. However, for this paper it was ran on a MacBook Air using a Windows emulator called CrossOver. Figure 20 shows the basic settings for 2Dshige©. A contour setting of 16 seemed to work best; any higher and the maps became over saturated, and any lower peaks are easily missed. Choosing a 100 setting on the x-axis caused the numbers

on the axis to run together. Therefore, a 200 division on the x-axis was chosen. After selecting a spectrum and drawing the map, simply click the copy button and then paste the map into another program. Peaks on the maps can be found by moving the cursor over them; 2Dshige© displays the coordinates on the bottom of the program.

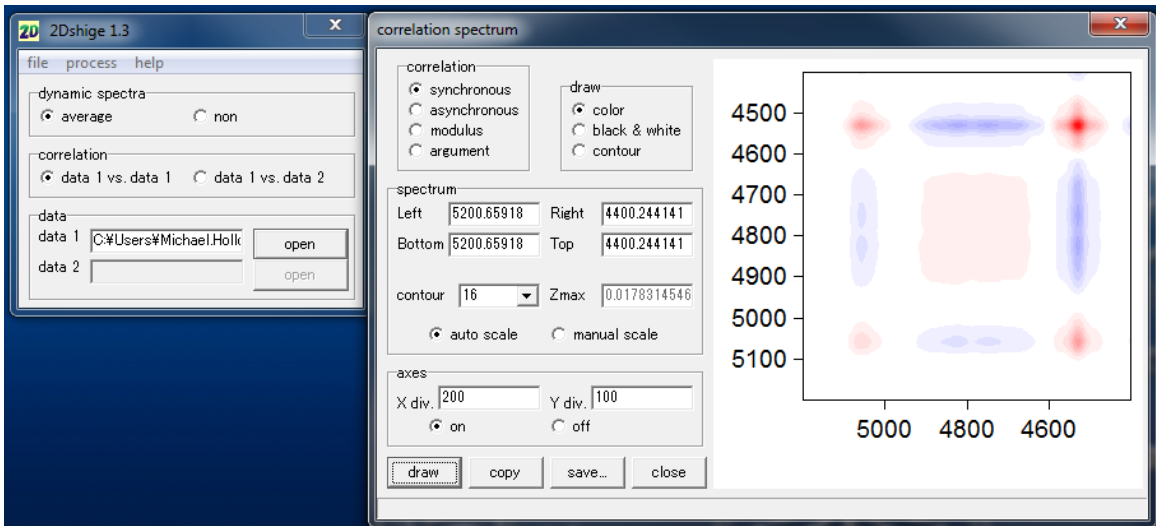

Figure 20. 2Dshige(c) program settings.

Common Errors

Below is a listing of errors commonly encountered when first using 2Dshige©.

Floating point error:

Microsoft Excel 2011 for Mac seemed to add metadata to the worksheet when it is saved as a CSV file, which caused 2Dshige© to crash due to floating point errors. Therefore, the CSV data files were created using Google Documents. After calculating all of the values in Excel, the values (not the formulas) were copied into Google Documents online and the document saved as a CSV file. This process eliminated the frustrating floating point errors. Microsoft Excel for Windows did not seem to have this problem.

I/O Error 32:

Having the CSV file open elsewhere while you attempt to run 2Dshige© will cause this error.

“Ink Blot” error:

If the data looks unreadable, too saturated, or has only a few very tiny peaks, adjust the scale of the axis to a smaller region.